



Calculation and Analysis of Groove Elastic Support's Radial Stiffness

X. Sun^{a,b}, S. Deng^{b,c}, G. Chen^a, W. Zhang^a

^a School of Mechatronics Engineering, Northwestern Polytechnical University, Xi'an, China

^b School of Mechatronics Engineering, Henan University of Science and Technology, Luoyang, China

^c Collaborative Innovation Center of Major Machine Manufacturing in Liaoning, Liaoning, China

PAPER INFO

Paper history:

Received 05 January 2017

Received in revised form 21 March 2017

Accepted 21 April 2017

Keywords:

Groove Elastic Support
Analysis Formula
Radial Stiffness
Structure Parameter
Stiffness Homogeneity

ABSTRACT

In this paper, an analytical formula to calculate the radial stiffness of groove elastic support is presented. The influence of structure parameters on radial stiffness and homogeneity of radial stiffness is investigated as well. The accuracy and calculating speed of the analysis formula are compared to that of finite element method (FEM). Findings are as following: The calculating speed of analysis formula is more efficient than that of finite element method (FEM). When the number of groove is less than 20, the maximum relative error of two methods is less than 10%. The radial stiffness of groove elastic support increases with the groove number, thickness of arc beam and transition angle, but decreases with the groove gap. The radial stiffness changes slightly and periodically with the azimuth angle of radial load, and the greater groove number and the thinner thickness of arc beam, the more homogeneous radial stiffness of groove elastic support.

doi: 10.5829/ije.2017.30.07a.16

1. INTRODUCTION

In high speed rotor with the determined design scheme, it is difficult to adjust the critical speed of rotor system through changing the structure dimension [1, 2], whereas installing the elastic support with lower stiffness on the rotor system can easily reduce the critical speed and realize the rotor to be safely operated over the critical speed [3-6]. Therefore, the structure design and stiffness calculation of elastic support has become the interest to many researchers.

The stiffness formulas of typical elastic support, such as elastic ring, squirrel cage elastic, etc., based on mechanics of material theory and deduced from simplified models, are still widely used for the initial designing of typical elastic support. Ecsedi et al. [7] proposed the formulas of the torsional rigidity of the elastic ring, applying the usual assumptions of linear theory of elasticity and the Michell's theory. As stated in literature [8], an expression for the radial displacement has been derived for a thin elastic ring loaded by any combination of radial, tangential and moment loads in

its plane. Dai Jianxing [9] derived the elastic ring's stiffness coefficient, and compared the result by proposed formula with that by finite element method (FEM) and the test value of stiffness shows that this analysis method is available. Cao Lei [10, 11] and Zhang Wei [12] investigated the stiffness characteristics of corrugated elastic ring by finite element method (FEM) and found that the characteristics-contact status of this elastic ring is the important factor adjusting the rotor critical speed and the deformation of this elastic ring can moderate nonlinear characteristics of elastic ring squeeze film damper (ERSFD). Hong Jie [13] adopted finite element method (FEM) to investigate the characteristics of a gas turbine engine with ERSFD and found the deformation of the elastic ring can adjust the oil film clearance. In literature [14], a metal mesh damper was designed and static stiffness was tested under different working conditons. The experimental results show that the metal mesh damper has stable support performance. Ma Yanhong [15] also used finite element method (FEM) to study an elastic ring-metal rubber damper and get the elastic support properties. Zou et al. [16] investigated the deformation and mechanical response of a rubbery metallic material and

*Corresponding Author's Email: 64354106@qq.com (X. Sun)

analyzed the mesoscopic structural properties of the material and its evolution during part producing. In order to improve accuracy of support stiffness design for squirrel cage elastic support and reduce the maximal stress of squirrel cage into capacity, Wang et al. [17] proposed a kind of optimization design method based on the finite element optimization techniques. To enhance the calculation efficiency of finite element method (FEM). In this paper, the groove elastic support belongs to elastic ring. Deng et al. [18] studied the effect of structural parameters of groove elastic support on vibration characteristics of the rolling bearing combining rigid and flexible coupled method, the result shows magnitude of inner vibration can be significantly decreased with the elastic support, but the research do not refer to the stiffness calculation of the elastic support. The above mentioned research mainly focus on the stiffness calculation and structure optimizing design of corrugated elastic ring and squirrel cage elastic support. However, the study on the stiffness and structural design of the groove elastic support has not been around researcher's interest, especially the radial stiffness of groove elastic support.

In this paper, the analytical formulas of groove elastic support's radial stiffness are built based on mechanics of material theory, and then the calculation results are validated by finite element method (FEM). The findings provide a theoretical basis for the calculation of radial stiffness and designing of groove elastic support.

2. ANALYTICAL METHOD OF RADIAL STIFFNESS FOR GROOVE ELASTIC SUPPORT

2.1. Structure of Groove Elastic Support The groove elastic support is an atypical elastic support, which is mounted between the house and bearing's outer ring with an interference fit. The assembly diagram of groove elastic support is shown in Figure 1. The structure and deformation of groove elastic support are illustrated in Figure 2.

In Figure 1, inertial coordinate system $\{O; X, Y, Z\}$ is fixed in the space, X axis coincides with bearing rotating axis, YOZ plane parallels the bearing radial plane passing through bearing center, and ω_i is angular velocity of inner ring. In Figure 2 (a), D_i and D_o are the inner and outer diameters of elastic support respectively; H is thickness of the arc beam, H' the groove gap, α transition angular, A point and B point are the ends of the pth arc beam, ϵ_p the azimuth angle of the pth arc beam that is the angle from the end B of arc beam to the negative half Y axis along counterclockwise direction. In Figure 2 (b), the initial position of coordinate system of elastic support center $\{O_T; X_T, Y_T, Z_T\}$ coincides with $\{O; X, Y, Z\}$, and

$\{O_T; X_T, Y_T, Z_T\}$ does not rotate but just translate in YOZ plane, δ is the radial displacement of elastic support center O_T , y_o and z_o are the displacement component of δ along Y and Z axis, respectively; γ is the angle between $\{O_T; X_T, Y_T, Z_T\}$ and $\{O; X, Y, Z\}$; L is the width of the elastic support.

2.2. Analytic Formula of Radial Stiffness In order to establish the model of elastic support's radial stiffness, the following hypotheses are proposed:

- (1) Compared with groove elastic support, outer ring of bearing is considered as a rigid body and just has a rigid displacement in OYZ plane.
- (2) When the arc beam of groove elastic support bends with the radial force, the ends of arc beam A and B have no angular displacement.
- (3) The bending deformation of arc beam belongs to the local small deformation which has no influence on the global dimension of groove elastic support.

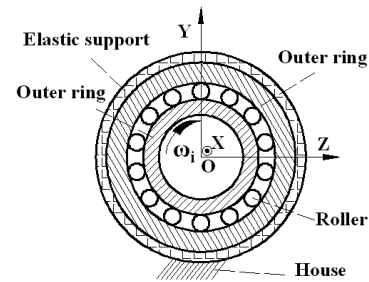
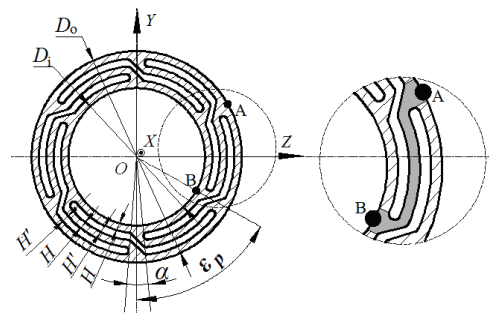
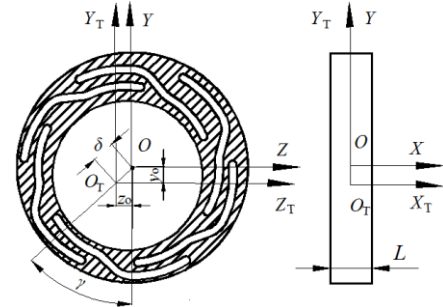


Figure 1. Assembly diagram of groove elastic ring assemble



(a) Schematic structure of groove elastic support



(b) Deformation and coordinate of elastic support

Figure 2. Schematic diagram of elastic support structure and deformation

The force and deformation on the end B of the pth arc beam in OYZ plane are shown in Figure 3. Because of interference fit between groove elastic support and bearing housing, the end A of arc beam is considered to be fixed. The other end B of arc beam moves to B' point due to a radial force, and the displacement of B' point is δ , which is also the displacement of outer ring's centroid.

The meaning and expression of parameters in Figure 3 are shown in Table 1

Due to the hypotheses without angular displacement at the end B, the moment M_p is neglected, and the inner forces at the end B can be written as follows, according to the elastic center method in literature [19].

$$\left\{ \begin{aligned} f_{\xi p} &= -\frac{a_p}{\int_{-\frac{\phi}{2}}^{\frac{\phi}{2}} \frac{(\eta-\eta_s)^2}{EI} ds + \int_{-\frac{\phi}{2}}^{\frac{\phi}{2}} \frac{\cos^2 \varphi}{EA_s} ds + \int_{-\frac{\phi}{2}}^{\frac{\phi}{2}} \frac{\mu \sin^2 \varphi}{GA_s} ds} \\ f_{\eta p} &= -\frac{b_p}{\int_{-\frac{\phi}{2}}^{\frac{\phi}{2}} \frac{\xi^2}{EI} ds + \int_{-\frac{\phi}{2}}^{\frac{\phi}{2}} \frac{\sin^2 \varphi}{EA_s} ds + \int_{-\frac{\phi}{2}}^{\frac{\phi}{2}} \frac{\mu \cos^2 \varphi}{GA_s} ds} \end{aligned} \right. \quad (1)$$

In Equation (1), μ is material shear factor (for the rectangular cross section μ is 1.2), E material elastic modulus, G material shear modulus, I the inertia moment of cross-section, $I = LH^3/12$, (ξ, η) the coordinate of arbitrary point on the arc beam in $\{\xi_p, C_p, \eta_p\}$, $\xi = R \sin \theta$, $\eta = R(1 - \cos \theta)$; $ds = R d\theta$; A_s

the area of cross-section, $\eta_s = \int_{-\frac{\phi}{2}}^{\frac{\phi}{2}} \frac{\eta}{EI} ds / \int_{-\frac{\phi}{2}}^{\frac{\phi}{2}} \frac{1}{EI} ds$.

In Figure 4, the internal forces of point B are decomposed in $\{O; X, Y, Z\}$, ζ_p is the included angle between Y axis and the chord direction of the pth arc beam, and z_o and y_o are the components of δ and can be calculated by Equation (2).

$$\left\{ \begin{aligned} z_o &= -\delta \sin \gamma \\ y_o &= -\delta \cos \gamma \end{aligned} \right. \quad (2)$$

TABLE 1. Parameters' meaning and expression in Figure 3

$\{\xi_p, C_p\}$	local coordinate system of the pth arc beam
η_p	midpoint of arc beam
C_p	midpoint of arc beam
ξ_p	tangential direction of the arc beam
η_p	perpendicular to ξ_p axis
R	radius of the arc beam $R=D_i/2+3H/2+H'$
Φ	span angle of arc beam
φ	included angle between the tangent of an arbitrary point on arc beam and the chord of arc beam
β_p	included angle between the line BB' (δ) and the η_p axis
a_p, b_p	$a_p = \delta \sin \beta_p$, $b_p = \delta \cos \beta_p$
$f_{\xi p}, f_{\eta p}, M_p$	internal forces and moment of B point
η_s	elastic center of arc beam

Supposing ε_1 is the azimuth angle of the first arc beam, span angle ϕ can be written as $\phi = 2\pi/n - \alpha/2$, n is the number of arc beam.

The relationships of the geometric parameters are shown as Equation (3).

$$\left\{ \begin{aligned} \varepsilon_p &= \varepsilon_1 + 2(p-1)\pi/n \\ \zeta_p &= \frac{\pi}{2} - \left(\frac{\phi}{2} + \varepsilon_p \right) \\ \beta_p &= \pi - \left(\gamma + \varepsilon_p + \frac{\phi}{2} \right) \\ \gamma &= \arctan \frac{z_o}{y_o} \end{aligned} \right. \quad (3)$$

The components of the internal forces at B point in $\{O; X, Y, Z\}$ are shown as Equation (4).

$$\left\{ \begin{aligned} F_{yp} &= f_{\eta p} \sin \zeta_p - f_{\xi p} \cos \zeta_p \\ F_{zp} &= -f_{\eta p} \cos \zeta_p - f_{\xi p} \sin \zeta_p \end{aligned} \right. \quad (4)$$

Since the outer ring is without rotation, it is not necessary to calculate the moment, and then the force components of outer ring through groove elastic support are shown as Equation (5), according to the force interaction theory.

$$\left\{ \begin{aligned} F_y &= -\sum_{p=1}^n F_{yp} \\ F_z &= -\sum_{p=1}^n F_{zp} \end{aligned} \right. \quad (5)$$

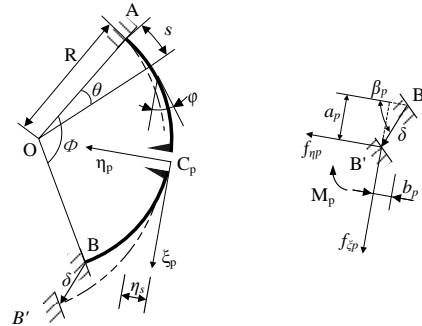


Figure 3. Schematic diagram of arc beam deformation and force in local coordinate system

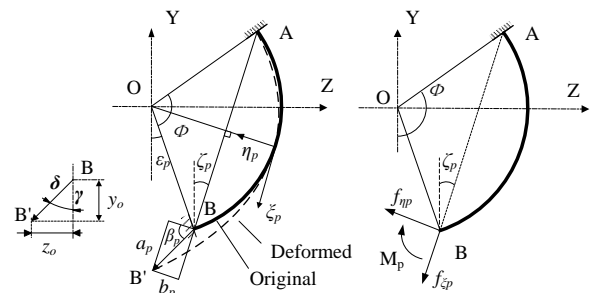


Figure 4. Deformation and forces of arc beam

Substituting Equation (1)-(4) into Equation (5), the following expression is obtained.

$$\begin{cases} F_z = \sqrt{y_0^2 + z_0^2} \sum_{p=1}^n \left[\frac{\sin \beta_p}{\Gamma} \cos \zeta_p - \frac{\cos \beta_p}{\Lambda} \sin \zeta_p \right] \\ F_y = \sqrt{y_0^2 + z_0^2} \sum_{p=1}^n \left[\frac{\sin \beta_p}{\Gamma} \sin \zeta_p + \frac{\cos \beta_p}{\Lambda} \cos \zeta_p \right] \\ \Gamma = \int_{-\frac{\phi}{2}}^{\frac{\phi}{2}} \frac{(\eta - \eta_s)^2}{EI} ds + \int_{-\frac{\phi}{2}}^{\frac{\phi}{2}} \frac{\cos^2 \varphi}{EA_s} ds + \int_{-\frac{\phi}{2}}^{\frac{\phi}{2}} \frac{\mu \sin^2 \varphi}{GA_s} ds \\ \Lambda = \int_{-\frac{\phi}{2}}^{\frac{\phi}{2}} \frac{z^2}{EI} ds + \int_{-\frac{\phi}{2}}^{\frac{\phi}{2}} \frac{\sin^2 \varphi}{EA_s} ds + \int_{-\frac{\phi}{2}}^{\frac{\phi}{2}} \frac{\mu \cos^2 \varphi}{GA_s} ds \end{cases} \quad (6)$$

The radial stiffness of groove elastic support can be written as Equation (7).

$$K = \frac{F_y \cos \gamma + F_z \sin \gamma}{\delta} \quad (7)$$

Substituting Equation (2) and Equation (6) into Equation (7), gives the following expression:

$$\begin{aligned} K = \cos \gamma \sum_{p=1}^n \left[\frac{\sin \beta_p}{\Gamma} \sin \zeta_p + \frac{\cos \beta_p}{\Lambda} \cos \zeta_p \right] \\ + \sin \gamma \sum_{p=1}^n \left[\frac{\sin \beta_p}{\Gamma} \cos \zeta_p - \frac{\cos \beta_p}{\Lambda} \sin \zeta_p \right] \end{aligned} \quad (8)$$

3. FINITE ELEMENT MODEL OF GROOVE ELASTIC SUPPORT

In order to verify the accuracy of the proposed analytic formula, the finite element model of the elastic support in Figure 5 was built in ANSYS software. It is assumed that the material is linear, and there is no plastic deformation under radial load. The finite element model is 2D with plane182 element. The mesh size is 0.5mm, the areas near the transition angles are meshed by 0.05mm. The outer surface of the elastic support is fixed in the space. All degrees of freedom of nodes on the surface are coupled to the center of the inner surface of groove elastic support, where a radial load (F_r) is applied on.

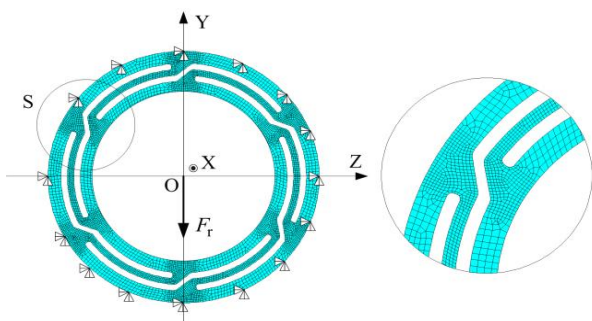


Figure 5. Finite element model of groove elastic ring

After FEM solution, the radial displacement δ of the inner surface of groove elastic supports can be obtained, and then the radial stiffness K can be written as Equation (9).

$$K = \frac{F_r}{\delta} \quad (9)$$

4. COMPARISONS AND ANALYSIS BETWEEN TWO METHODS

The material of groove elastic support is 8Cr4Mo4V, and the main structural parameters are shown in Table 1. According to Figure 1, the groove number n , arc beam thickness H , groove span H' and transition angle α were chosen to investigate the radial stiffness of groove elastic support.

4. 1. Influence of Groove Number on Radial Stiffness

The results of radial stiffness with different groove number n are shown in Figure 6, where T represent the analytic formula and F represent the FEM, respectively. The other structural parameters are the same values in Table 1. The radial load F_r is 500N. Considering the carrying capacity of the support, the least groove number is 12.

In Figure 6, it can be seen that the radial stiffness for two methods increases with the groove number n .

TABLE 1. Main structural parameters of groove elastic support

Parameters	Value
Inner diameter D_o /mm	150
Outer diameter D_i /mm	140
Axial width L /mm	19
Thickness of arc beam H /mm	0.5
Groove gap H' /mm	0.5
Transition angle α /°	2

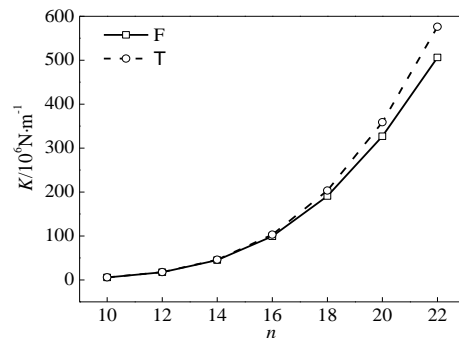


Figure 6. Radial stiffness under different groove number

The maximum of radial stiffness is less than 6.5 times the minimum when n changes from 12 to 22, and the radial stiffness calculated by the analytic formula is bigger than that calculated by FEM. The relative error between two methods increases with the groove number n , and the relative error is lower than 10% when n is less than 22.

4. 2. Influence of Groove Gap on Radial Stiffness

The radial stiffness with different groove gap H' is shown in Figure 7. The other structural parameters are the same values in Table 1. The radial load F_r is 500N. In Figure 7, the changing trends of radial stiffness by two methods are identical, and the radial stiffness decreases with the groove gap H' . When H' changes from 0.4 mm to 1.4 mm, the radial stiffness varies in a narrow range which is less than 2%. The stiffness calculated by analytic formula is slightly higher than the value calculated by FEM. Meanwhile, the less groove number, the less relative error induced by the groove gap. When $n \leq 22$ and $H' \leq 1.2\text{mm}$, the relative error between two methods is less than 10%.

4. 3. Influence of Beam Thickness on Radial Stiffness

The radial stiffness with different beam thickness H is shown in Figure 8. The other structural parameters are the same values in Table 1. The radial load F_r is 500N. In Figure 8, the radial stiffness by two methods increases with the groove gap H . The maximum of radial stiffness is less than 7.6 times the minimum when H changes from 0.4 mm to 1.2 mm. The radial stiffness calculated by analytic formula is slightly higher than that calculated by FEM. When $H \leq 1.2\text{mm}$ and $n \leq 20$, the relative error between two methods is less than 10%.

4. 4 Influence of Transition Angle on Radial Stiffness

The radial stiffness with different transition angle α are shown in Figure 9. The other structural parameters are the same values in Table 1.

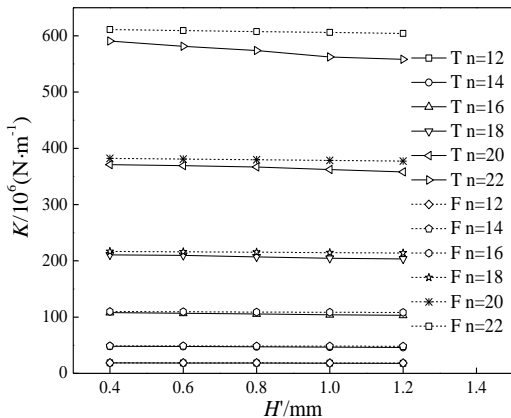


Figure 7. Radial stiffness under different groove gap

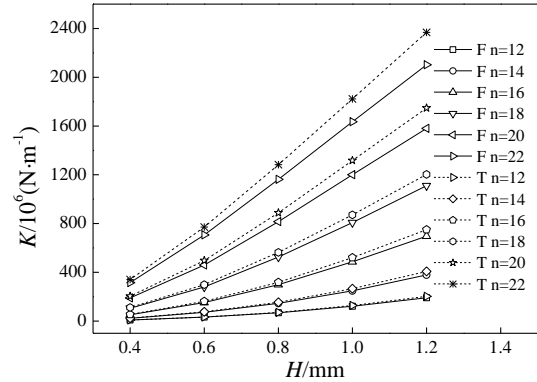


Figure 8. Radial stiffness under different arc beam thickness

The radial load F_r is 500N. In Figure 9, the radial stiffness increases with the transition angle, and the maximum of radial stiffness is less than 1.36 times the minimum when α changes from 2.0° to 4.0° . The radial stiffness calculated by analytic formulation is slightly higher than that calculated by FEM. The less transition angle, the less relative error between two methods. When $\alpha \leq 4^\circ$ and $n \leq 20$, the relative error is less than 10%.

5. INFLUENCE OF STRUCTURAL PARAMETERS ON THE STIFFNESS HOMOGENEITY OF GROOVE ELASTIC SUPPORT

Due to groove elastic support with a cycle-symmetry structure along the circumferential direction, the radial stiffness changes periodically with the azimuth angle of radial load. In order to assess the homogeneity of radial stiffness, K'_i is defined as Equation (10). According to the previous analysis, groove number and arc beam thickness significantly influenced the stiffness of the support. So, in Equation (10), subscript i can be n or H . For a certain i , $K_{i\min}$ presents the minimum value of the different radial stiffness.

$$K'_i = K_i / K_{i\min} \tag{10}$$

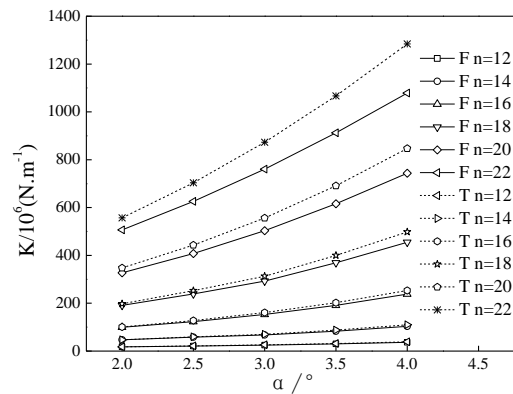


Figure 9. Radial stiffness under different transition angle

5. 1. Influence of Groove Number on Stiffness Homogeneity

In Figure 10, the homogeneity of radial stiffness changes periodically with azimuth angle of radial load. The structural parameters are the same values in Table 1. The radial load F_r is 500N. Under different azimuth angle of radial load, the variation period of radial stiffness is $2\pi/n$. The values of K'_n are all less than 1.000035. The more groove number, the better homogeneous radial stiffness.

5. 2. Influence of Arc Beam Thickness on Stiffness Homogeneity

The trend of homogeneity of radial stiffness with azimuth angle of radial load is shown in Figure 11. The structural parameters are the same values in Table 1. The radial load F_r is 500N. Because of periodic variation of elastic support stiffness, the change of stiffness homogeneity in one period is plotted in the following figures.

The stiffness homogeneity slightly declines with H . If the groove number is a multiple of 4, the stiffness increases first and then decreases, if not, the stiffness decreases first and then increases with the change of load direction.

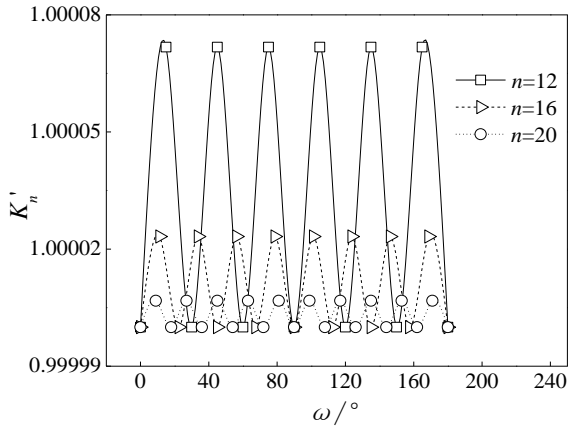
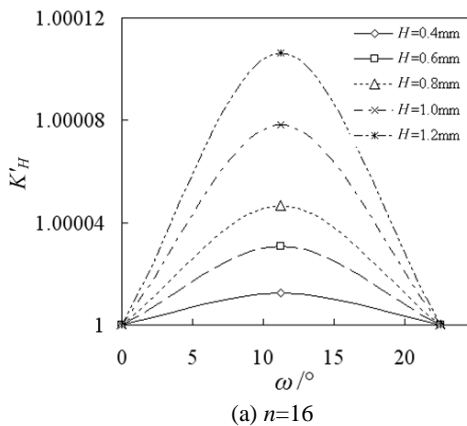
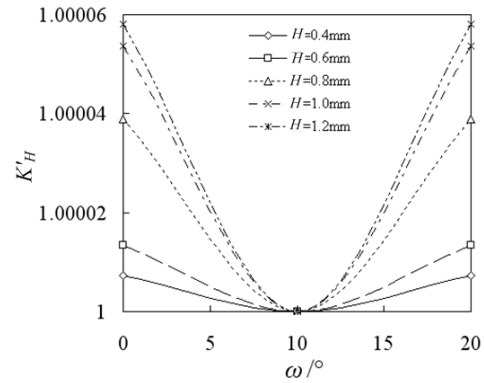


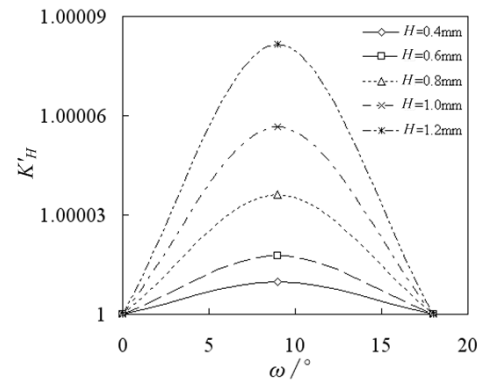
Figure 10. Influence of azimuth angle on radial stiffness under different groove number



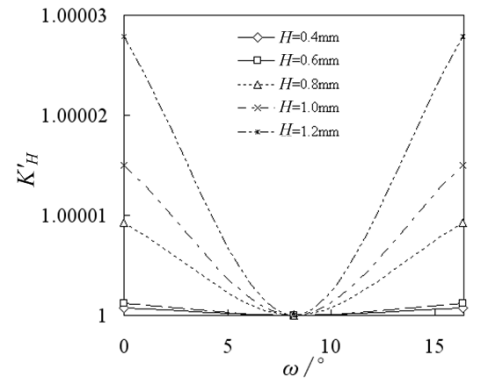
(a) $n=16$



(b) $n=18$



(c) $n=20$



(d) $n=22$

Figure 11. Influence of load azimuth angle on radial stiffness under different arc beam thickness

6 CONCLUSIONS

In this paper, all calculations were carried out on the computer with forty Inter(R) Xeon(R) CPU and 192GB of memory. The calculation of analytic formulation spends 0.02s, but FEM needs to more than 30min. The conclusions are:

- (1) When the groove number is less than 20, arc beam thickness and groove gap change from 0.4mm to 1.2mm, and the transition angle changes from 2° to 4° ,

the relative error of radial stiffness between two methods is less than 10%.

(2) The radial stiffness of groove elastic support increases with the groove number, thickness of arc beam and transition angle, but slightly decreases with the groove gap.

(3) The radial stiffness of groove elastic support changes periodically with the azimuth angle of radial load, but the variation range is small. The greater groove number and smaller thickness of arc beam, the better homogeneity of radial stiffness.

7. ACKNOWLEDGMENTS

This paper has been financially supported by National Natural Science Foundation of China (U1404514), Henan Outstanding Person Foundation in China (144200510020) and the Collaborative Innovation Center of Major Machine Manufacturing in Liaoning, China.

8. REFERENCES

- Xu, W., Wen, Z., Xu, L., Liu, Y. and Shen, X., "High speed rotating test-bed with flexible, squeeze film damped support", *Jixie Gongcheng Xuebao(Chinese Journal of Mechanical Engineering)(China)*, Vol. 40, No. 9, (2004), 144-147.
- Dayi, Z. and Guoxin, M., "Hong jie beijing university of aeronautics and astronautics, beijing 100083, china; rigidity calculation methods for rotor supporting system in gas engine [j]", *Tactical Missile Technology*, Vol. 2, (2005), 143-150.
- Ahmadi, S.M., Ghazavi, M. and Sheikhzad, M., "Dynamic analysis of a rotor supported on ball bearings with waviness and centralizing springs and squeeze film dampers", *International Journal of Engineering-Transactions C: Aspects*, Vol. 28, No. 9, (2015), 1351-1360.
- Kirk, R.G. and Gunter, E.J., "The effect of support flexibility and damping on the dynamic response of a single mass flexible rotor in elastic bearings", (1972).
- Mahjouri, S., Shabani, R. and Rezazadeh, G., "Vibration analysis of an air compressor based on a hypocycloidal mechanism: An experimental study", *International Journal of Engineering-Transactions B: Applications*, Vol. 28, No. 11, (2015), 1687-1694.
- Kang, C., Hsu, W., Lee, E. and Shiau, T., "Dynamic analysis of gear-rotor system with viscoelastic supports under residual shaft bow effect", *Mechanism and Machine Theory*, Vol. 46, No. 3, (2011), 264-275.
- Ecsedi, I., "Bounds for the torsional rigidity of elastic ring", *Mechanics research Communications*, Vol. 26, No. 4, (1999), 445-450.
- Liu, J. and Chiu, Y., "Analysis of a thin elastic ring under arbitrary loading", *Journal of Engineering for Industry*, Vol. 96, No. 3, (1974), 870-876.
- Xingjian, D. and Guangming, W., "Analysis on stiffness of corrugated ring in a rotor-bearing support", *Journal of Harbin Institute of Technology*, (1994), 05-13.
- CAO, L., GAO, D.-p. and JIANG, H.-f., "Investigation on critical speed characteristics of elastic ring sfd-rotor system [j]", *Journal of Propulsion Technology*, Vol. 2, (2008), 20-29.
- Cao, L., Gao, D. and Jiang, H., "Damping mechanism of elastic ring squeeze film damper", *Journal of Vibration Engineering*, Vol. 6, (2007), 584-589.
- Zhang, W. and Ding, Q., "Elastic ring deformation and pedestal contact status analysis of elastic ring squeeze film damper", *Journal of Sound and Vibration*, Vol. 346, (2015), 314-327.
- Jie, H., Yin, D. and Dayi, Z., "Dynamic design method of elastic ring squeeze film damper", *Journal-Beijing University of Aeronautics And Astronautics*, Vol. 32, No. 6, (2006), 649-655.
- Zarzour, M.J., "Experimental evaluation of a metal-mesh bearing damper in a high speed test rig", Texas A&M University, (1999),435-442
- Hongwei, M.Y.L. and Haixiong, Z., "Hong jie school of jet propulsion, beihang university, beijing 100191, china; structural stiffness design and experimental evaluation of elastic ring-metal rubber damper [j]", *Acta Aeronautica et Astronautica Sinica*, Vol. 6, (2013), 723-730.
- Zuo, H., Bai, H. and Feng, Y., "The analysis of stiffness for rubbery metallic material based on mesoscopic features", *Materials Sciences and Applications*, Vol. 2, No. 06, (2011), 654-660.
- Wang, D., Zhang, W., Wang, Z. and Zhu, J., "Shape optimization of 3d curved slots and its application to the squirrel-cage elastic support design", *Science China Physics, Mechanics & Astronomy*, Vol. 53, No. 10, (2010), 1895-1900.
- Deng, S.-E., Yan, Y.-C., Wang, Y.-S. and Yang, H.-S., "Vibration analysis of two-piece inner ring angular contact ball bearing with elastic support", *Journal of Aerospace Power*, Vol. 28, No. 2, (2013), 241-251.
- Carpinteri, A., "Structural mechanics fundamentals, CRC Press, (2013).

Calculation and Analysis of Groove Elastic Support's Radial Stiffness

RESEARCH
NOTEX. Sun^{a,b}, S. Deng^{b,c}, G. Chen^a, W. Zhang^a^a School of Mechatronics Engineering, Northwestern Polytechnical University, Xi'an, China^b School of Mechatronics Engineering, Henan University of Science and Technology, Luoyang, China^c Collaborative Innovation Center of Major Machine Manufacturing in Liaoning, Liaoning, China

P A P E R I N F O

چکیده

Paper history:

Received 05 January 2017

Received in revised form 21 March 2017

Accepted 21 April 2017

Keywords:

Groove Elastic Support

Analysis Formula

Radial Stiffness

Structure Parameter

Stiffness Homogeneity

در این مقاله، یک فرمول تحلیلی برای محاسبه سختی شعاعی پشتیبان بلبرینگ ارائه شده است. سپس، اثر پارامترهای ساختاری بر سختی شعاعی و همگن بودن سختی شعاعی نیز مورد بررسی قرار گرفته است. دقت و سرعت محاسبه فرمول تحلیلی با روش المان محدود (FEM) مقایسه شده است. یافته‌ها به شرح زیر است: سرعت محاسبه فرمول تحلیلی کارایی بیشتری نسبت به روش المان محدود (FEM) دارد. هنگامی که تعداد شیارها کمتر از ۲۰ باشد، خطای حداکثر نسبی دو روش کمتر از ۱۰٪ است. سختی شعاعی شیارهای پشتیبان کش‌سان با تعداد شیار، ضخامت قوس و زاویه انتقال افزایش می‌یابد، اما با شکاف شیار کاهش می‌یابد. سختی شعاعی به طور دوره‌ای و به میزان کمی با زاویه آزیموت بار شعاعی تغییر می‌کند. هرچه تعداد شیارهای بزرگتر و ضخامت قوس نازک‌تر باشد، سختی شعاعی شیار پشتیبان کش‌سان یکنواخت‌تر است.

doi: 10.5829/ije.2017.30.07a.16